

Location of P and As dopants and p-type doping of ZnO

PAUL FONSA*, ALEXANDER V. KOLOBOV^a, JUNJI TOMINAGA^b, BÉRANGÈRE HYOT^c, BERNARD ANDRÉ^c

^a*Nanoelectronics Research Institute, National Institute of Advanced Industrial Science & Technology, Tsukuba Central 4, Higashi 1-1-1, Tsukuba, Ibaraki, 305-8562, Japan and SPring-8, Japan Synchrotron Radiation Institute (JASRI), Kouto 1-1-1, Sayo-cho, Sayo-gun, Hyogo 679-5148, Japan*

^b*Nanoelectronics Research Institute, National Institute of Advanced Industrial Science & Technology, Tsukuba Central 4, Higashi 1-1-1, Tsukuba, Ibaraki, 305-8562, Japan*

^c*CEA, LETI, MINATEC, F-38054 Grenoble, France*

Although ZnO has long been touted as an excellent material for UV light-emitting diodes and lasers, p-type doping still remains a challenge. In recent reports claiming that p-type doping can be achieved using nitrogen, arsenic and phosphorus, the spatial location of the dopants in the “successful” samples has not been identified. In this work, we present simulation results of x-ray absorption spectra for different locations of p-type dopants and argue that this technique is a powerful tool to experimentally investigate the location of group V dopants and to establish a correlation between the dopant location and corresponding conductivity type.

(Received December 5, 2013; accepted January 22, 2014)

Keywords: P + As dopants, P-type ZnO

Recently, there has been increased interest in zinc oxide (ZnO) semiconductor material, primarily determined by its prospects for optoelectronics applications owing to its wide direct band gap ($E_g=3.3$ eV at 300 K) and a large exciton binding energy of ca. 60 meV.

Before ZnO can be put in practical use for optoelectronic applications, a critical problem must be overcome, namely, the reliable growth of p-type-conductivity ZnO layers. There are two major approaches on the way to achieve this goal, one is to use substitutional (Zn-site) doping using group-I elements such as Li, Na, and K and the other is to use group-V acceptor dopants such as N, P, and/or As. In this work we discuss the case of the group-V dopants.

Density functional theory (DFT) predicts that phosphorus located on oxygen sites, P_O , should form a deeper acceptor level (0.93 eV), as compared with the value of 0.40 eV predicted for N_O [1] likely due to the difference in the ionic size mismatch between P and O; the As_O level is even deeper (1.15 eV). It has also been argued that the effect of dopants may be compensated by the creation of other defects, coined “hole killers” that have a low formation energy and thus form readily [2].

At the same time, experimentally, there have been several reports on the successful doping of ZnO by N, P, and As. For example, p-type doping by nitrogen was obtained using MBE [3, 4], CVD [5], and reactive magnetron sputtering [6]. Similarly, there also have been reports of successful p-type doping by other group-V elements. Aoki et al. [7] used laser doping of P (from Zn_3P_2) to produce a homojunction diode exhibiting light emission; the result implies that p-type ZnO was formed. Kim et al. [8] have claimed to have produced p-type ZnO with a resistivity of 0.6 Ohm-cm using P_2O_5 . Ryu et al. reported As-doped p-type ZnO using GaAs substrates as an arsenic source [9].

Despite all the apparent progress that has been recently made and the reports of p-type conductivity in ZnO films using various growth methods and various group-V dopant elements, a reliable and reproducible high quality p-type conductivity has not yet been achieved. Therefore, it remains one of the most topical issue in ZnO research today and a large fraction of the research efforts are directed to solve this issue. The interested reader is referred to recent reviews that describe various aspects of the current state of the problem (see e.g. [10]).

A combination of the simulated and experimental results suggests that either DFT results are inaccurate for ZnO, or the acceptor is not simply substitutional PO or AsO . It is thus crucial to develop a reliable method to identify the location of impurities inside the ZnO matrix.

While in some cases doping has been performed during growth, it is interesting to note that successful doping has also been reported using diffusion of dopants from the substrate [9]. This approach is particularly attractive for ZnO nanostructures such as nanowires because the surface-to-volume ratio becomes significantly larger leading to increased doping efficiency [11]. p-type doping of ZnO nanowires has also been reported using chemical vapor deposition with P as dopant [12]. P-type conductivity was demonstrated using gate-voltage dependent conductance measurements of single ZnO:P nanowires with field effect transistor configuration. However, the p-type conductivity was not stable and reverted to n-type a couple of months later [12], the conversion most likely associated with a change in the location of P dopant atoms in the ZnO matrix, which implies that in the p-type samples the dopants are not located on the energetically most favourable sites, i.e. the dopants in p-type ZnO may be in metastable positions.

It is thus important to identify the spatial location of the dopants in the successful samples, and, ideally, the

evolution of the local structure around the dopants during the p-type to n-type transformation. Since DFT simulations look for the lowest-energy configuration, the DFT solution for the local structure of dopants may not necessarily be that same as in the experimentally produced metastable p-type structures. A technique that has been successfully used to investigate the local structure around a particular element is x-ray absorption (XAS) when due to the presence of the surrounding atoms the absorption spectrum has characteristic features both in the vicinity of the absorption edge (x-ray absorption near-edge structure, XANES) and well above the edge (extended x-ray absorption fine structure, EXAFS).

EXAFS allows one to determine the number of the first-nearest neighbours, the interatomic distances, and the chemical nature of the first nearest neighbours, which would seem ideal, but the very low amount of P dopants in the samples results in a rather poor signal-to-noise ratio, especially at higher k-values making reliable determination of the local structure difficult. Using EXAFS for As-doped samples, this issue is further complicated by the rather strong background signal originating from Zn atoms, whose K-edge is located rather close to that of As. XANES features, on the other hand, have significantly larger intensity than that of corresponding EXAFS oscillations and can potentially be used even for very dilute samples. They have the additional advantage of sampling bond angles due to XANES three-dimensional sensitivity [13]. XANES measurements have been previously successfully applied to investigate the spatial location of N impurities, where it was concluded that nitrogen readily forms N₂ molecules inside ZnO but to the best of our knowledge no such studies have been performed for P and As dopants [14].

In order to validate the proposal to use XANES spectroscopy, in this work, we performed first-principle XANES simulations for different locations of P and As dopants inside ZnO and demonstrated that there are pronounced differences between different structures. We thus propose that x-ray spectroscopy may be a powerful and reliable technique to investigate the spatial location of P and As in successful and unsuccessful ZnO samples and consequently relate the spatial location of the dopants with p-type doping of ZnO.

First, we used density-functional based ab-initio simulations to obtain the structures of As- and P-doped ZnO with As and P atoms located on Zn and O sites as well as in octahedral and tetrahedral interstitials. For the latter, tetrahedral interstitials within the Zn and O sublattices were considered. The calculations were carried out on cell containing one dopant with the cell size of 72 atoms (73 atoms for the interstitial location of dopants) using the plane-wave code CASTEP [15, 16]. Such cell sizes generate structures with ca. 10^{21} cm⁻³ dopants. Ultra-soft pseudopotentials were used. The exchange term was evaluated using the local density approximation from the numerical results of Ceperley and Alder [17] as parameterized by Perdew and Zunger [18]. The charge density was calculated with a plane wave cutoff of 380 eV and a $3 \times 3 \times 2$ Monkhorst-Pack grid. For the relaxation

processes the Broyden, Fletcher, Goldfarb, and Shannon algorithm [19] was used to relax the atomic coordinates at 0 K within a supercell of fixed volume; the volume was fixed to reflect the experimentally determined density of ZnO.

The XANES spectra were calculated using the CASTEP-relaxed structures using the ab-initio real-space full multiple-scattering code FEFF9. FEFF9 is a fully relativistic, all-electron Green function code that utilizes a Barth-Hedin formulation for the exchange-correlation part of the potential and the Hedin-Lundqvist self-energy correction. In our FEFF calculations, the cluster radius was set to 9 Å around the central atom, which corresponds to about 100 atoms in the model. While the concentration of the dopants in the model substantially exceeds the experimental concentration, we believe that the presence of just one dopant atom in the cluster used for FEFF simulations justifies its use for the present purpose.

We start with the results of structural relaxations. In the upper panel of Fig. 1 we show the structure of undoped ZnO in two different projections (marked in the Figure), where Zn atoms are shown in gray and O atoms are shown in red. For the dopants, we show the structure in one of these two projections, namely, choosing the one that gives a better visualization of the structure. In the bottom of Fig. 1 we show the density of states (DOS) for undoped ZnO. The smaller value of the gap with respect to experiment is a result of the well known gap underestimation in DFT.

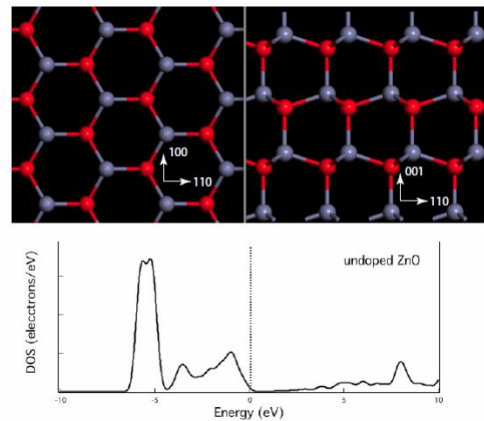


Fig. 1. Upper panel shows the structure of ZnO in two different projections. In the discussion below one of these projections is used. The lower panel shows DOS.

The results of the structural relaxation are shown in Figs 2-6. In the upper half we show the results for As and in the lower half for P dopants located in identical (prior to the lattice relaxation) positions. The panels on the left show the starting structure and the panels on the right show the relaxed structure. Arsenic atoms are shown in green and P atoms are shown in yellow. Under the structural models, the local DOS on the dopant atoms for the relaxed structures are shown.

In Fig. 2-3 the results for substitutional location of the dopants are shown. One can see that for both dopants the structural relaxation is minimal and for the dopants located on O sites (Fig. 3), p-type conductivity is expected.

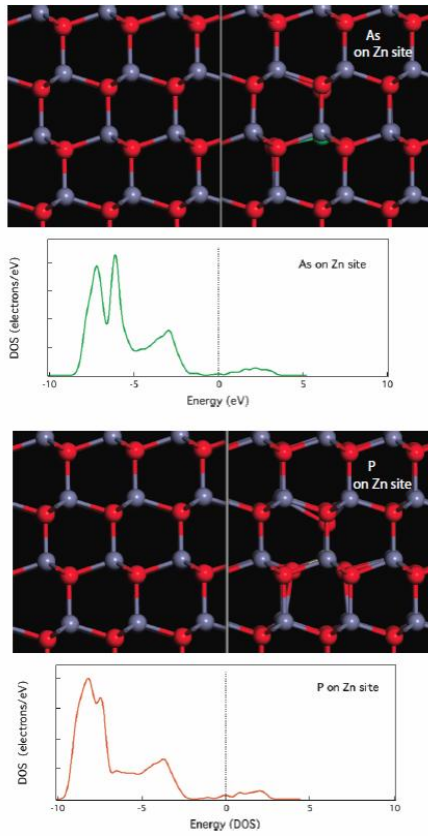


Fig. 2. The upper half corresponds to As dopant and the lower part corresponds to P dopants located on Zn sites. In these, the upper panel shows the starting (left) and relaxed (right) structures. The lower panel shows the local DOS on the dopant atom.

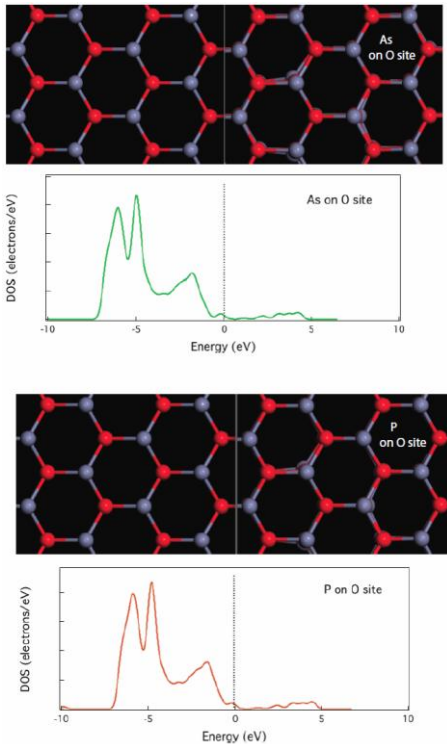


Fig. 3. The upper half corresponds to As dopant and the lower part corresponds to P dopants located on O sites. In these, the upper panel shows the starting (left) and relaxed (right) structures. The lower panel shows DOS.

Fig. 4 shows the result for dopants located on octahedral interstitials. Interestingly, p-type conductivity can be expected from P dopants but not from As dopants. Finally, dopants located on tetrahedral interstitials have been analysed. As noted earlier, there are two kinds of tetrahedral interstitials, namely those associated with the Zn sublattice and with the O sublattice.

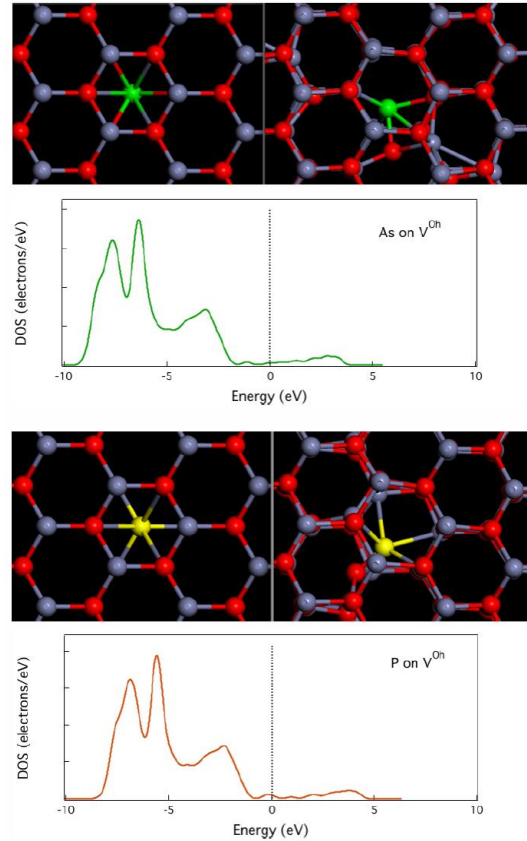


Fig. 4. The upper half corresponds to As dopant and the lower part corresponds to P dopants located on octahedral interstitials. In these, the upper panel shows the starting (left) and relaxed (right) structures. The lower panel shows DOS.

The two cases have been analysed separately and the results are shown in Figs 5 and 6. It should be noted that the lattice relaxation associated with tetrahedral location of dopants is very large, suggesting that when the material is doped experimentally, it is rather unlikely that the dopants occupy these positions in the lattice.

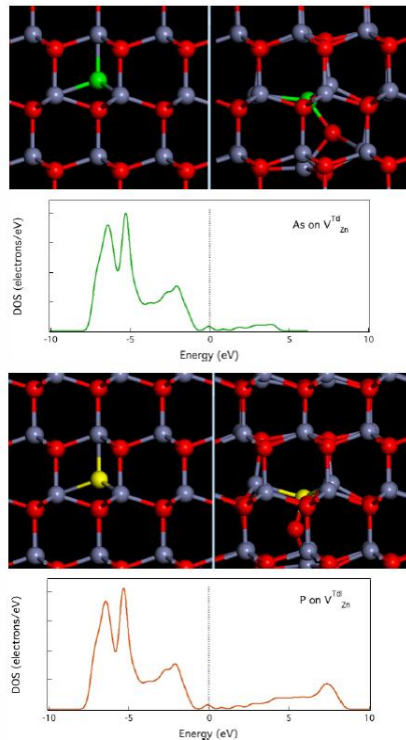


Fig. 5. The upper half corresponds to As dopant and the lower part corresponds to P dopants located on interstitials associated with the Zn sublattice. In these, the upper panel shows the starting (left) and relaxed (right) structures. The lower panel shows DOS.

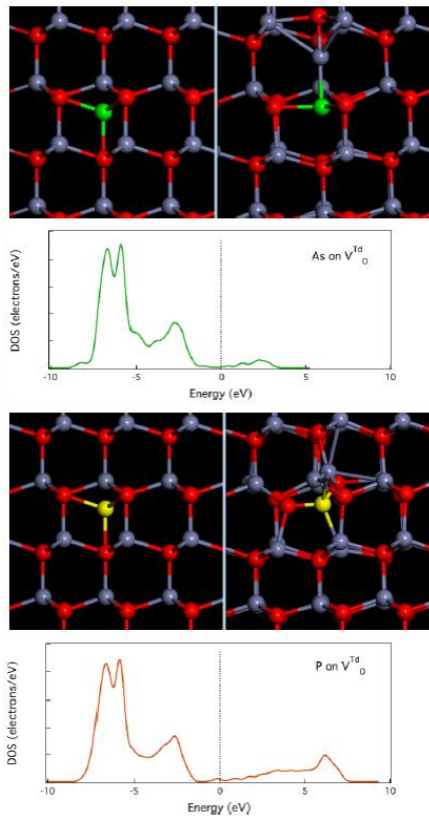


Fig. 6. The upper half corresponds to As dopant and the lower part corresponds to P dopants located on tetrahedral interstitials associated with the O sublattice. In these, the up-per panel shows the starting (left) and relaxed (right) structures. The lower panel shows DOS.

We now proceed to the results of XANES simulations. In Fig. 7 we show the simulated XANES spectra for all location of dopants described earlier. Two interesting aspects can be easily noticed. One is the striking similarity between the As- and P-XANES spectra for similar locations of the impurities. Thus for both kind of dopants located on O sites, the white line (the first intense feature in the spectrum) has an intensity about 1.6–1.8 \times higher than the intensity of the rest of the spectrum. In both cases, there is a pre-peak shoulder and the white line itself consists for three features better resolved in the P-XANES spectrum. The white line is followed by two similarly shaped features at higher energy. On the other hand, the spectra for the impurities located on Zn site are characterized by a very intense white line with a double-split feature above it. The XANES spectra for the interstitial dopants also look rather similar. Since the features in the XANES spectra are due to resonances in the electronic structure, the observed similarity demonstrates that both dopants generate similar energy levels (scaled with the absorption edge energy) and suggest that the two should generate similar electronic properties.

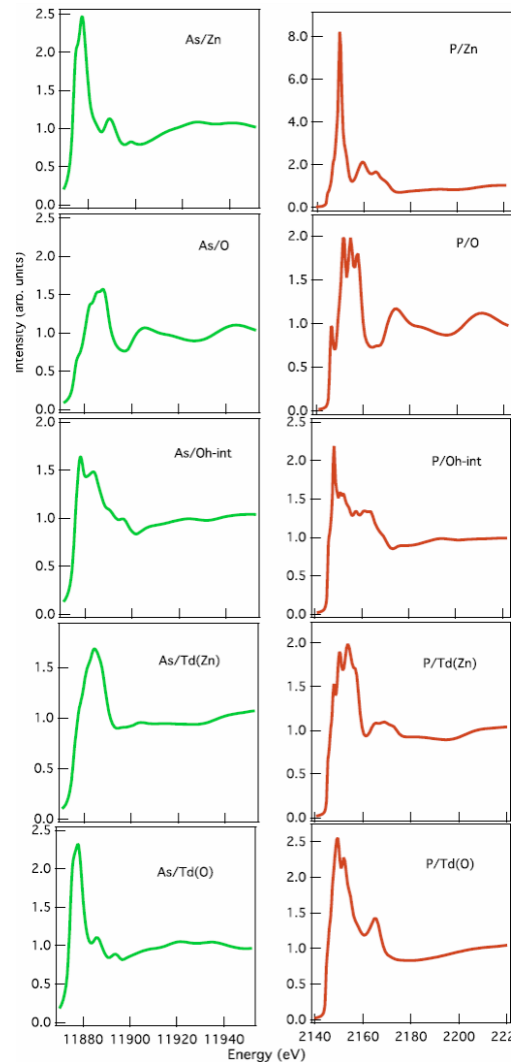


Fig. 7. Simulated XANES spectra for As (left) and P (right) dopants for different spatial location of dopants (marked in each panel).

Another interesting observation is that the spectra significantly differ among the different spatial locations of the dopants. Previously, XANES analysis has been successfully used to identify spacial location of impurities in crystals, e.g. in N-doped ZnO [14], or different local.

References

- [1] C. H. Park, S. B. Zhang, S. H. Wei, *Phys. Rev. B* **66**, 073202 (2002).
- [2] S. Zhang, S.-H. Wei, A. Zunger, *Phys. Rev. B* **63**, 075205 (2001).
- [3] D. C. Look, D. C. Reynolds, C. W. Litton, R. L. Jones, D. B. Eason, and G. Cantwell, *App. Phys. Lett.* **81**, 1830(2002).
- [4] A. B. M. Ashrafi, I. Suemune, H. Kumano, and S. Tanaka, *Jpn. J Appl. Phys.* **41**, L1281 (2002).
- [5] K. Minegishi, Y. Koiwai, Y. Kikuchi, K. Yano, M. Kasuga, and A. Shimizu, *Jpn. J. Appl. Phys.* **36**, L1453 (1997).
- [6] J. Lu, Y. Zhang, Z. Ye, L. Wang, B. Zhao, and J. Huang, *Mater. Lett.* **57**, 3311(2003).
- [7] T. Aoki, Y. Hatanaka, and D. C. Look, *Appl. Phys. Lett.* **76**, 3257(2000).
- [8] K.-K. Kim, H.-S. Kim, D.-K. Hwang, J.-H. Lim, and S.-J. Park, *Appl. Phys. Lett.* **83**, 63(2003).
- [9] Y. Ryu, S. Zhu, D. C. Look, J. M. Wrobel, H. M. Jeong, and H. W. White, *J. Cryst. Growth* **216**, 330(2000).
- [10] U. Ozgur, Y. I. Alivov, C. Liu, A. Teke, M. Reshchikov, S. Dogan, V. Avrutin, S.-J. Cho, and H. Morkoc, *J. Appl. Phys.* **98**, 041301(2005).
- [11] C. X. Shan, Z. Liu, C. C. Wong, and S. K. Hark, *J. Nanosci. and Nanotech.* **7**, 700(2007).
- [12] B. Xiang, P. Wang, X. Zhang, S. A. Dayeh, D. P. Aplin, C. Soci, D. Yu, and D. Wang, *Nano letters* **7**, 323(2007).
- [13] G. Smolentsev, A. V. Soldatov, and M. C. Feiters, *Phys. Rev. B* **75**, 144106(2007).
- [14] P. Fons, H. Tampo, A. Kolobov, M. Ohkubo, S. Niki, J. Tominaga, R. Carboni, F. Boscherini, and S. Friedrich, *Phys. Rev. Lett.* **96**, 045504(2006).
- [15] S. Clark, M. Segall, C. Pickard, P. Hasnip, M. Probert, K. Refson, M. J. Gill, *Phys. Rev. Lett.* **95**, 085503(2005).
- [16] M. Segall, P. J. D. Lindan, M. Probert, C. Pickard, P. Hasnip, S. Clark, and M. Payne, *J. Phys. Cond. Mat.* **24**, 2717(2002).
- [17] D. Ceperley and B. Alder, *Phys. Rev. Lett.* **45**, 566(1980).
- [18] J. Perdew and A. Zunger, *Phys. Rev. B* **23**, 5048(1981).
- [19] D. Johnson, *Phys. Rev. B* **38**, 12807 (1988).
- [20] M. Krbal, A. V. Kolobov, P. Fons, J. Tominaga, S. R. Elliott, J. Hegedus, and T. Uruga, *Phys. Rev. B* **83**, 054203(2011).
- [21] M. Krbal, A. V. Kolobov, P. Fons, K. V. Mitrofanov, S. R. Elliott, and J. Tominaga, *Appl. Phys. Lett.* **102**, 111904(2013).

*Corresponding author: paul-fons@aist.go.jp